



## Original articles

# Fitting thermal conductivity and optimizing thermoelectric efficiency in $Si_cGe_{1-c}$ nanowires

P. Rogolino<sup>a</sup>, V.A. Cimmelli<sup>b,\*</sup><sup>a</sup> *Department of Mathematical and Computer Sciences, Physical Sciences and Earth Sciences, University of Messina, Viale F. Stagno d'Alcontres, 31, 98166, Messina, Italy*<sup>b</sup> *Department of Mathematics, Computer Science and Economics, University of Basilicata, Viale dell'Ateneo Lucano, 10, 85100, Potenza, Italy*

Received 21 May 2019; received in revised form 11 September 2019; accepted 27 September 2019

Available online xxx

**Abstract**

We consider a thermoelectric energy generator constituted by a  $Si/Ge$  nanowire of length  $L$ . The dependence on composition and temperature of its thermal conductivity is analyzed in view of three series of experimental data obtained at the constant temperatures  $T = 300K$ ,  $T = 400K$ , and  $T = 500K$ . The best-fit curve is determined by a nonlinear regression method (NLRM). Then, under the hypothesis of nonlinear constitutive equation for the heat flux, we investigate the thermoelectric efficiency of the system as function of the composition of the nanowire and of the difference of temperature applied to its ends. For each temperature we calculate the value of the composition which realizes the optimal efficiency of the thermoelectric energy conversion. The corresponding value of the thermal conductivity is determined as well.

© 2019 International Association for Mathematics and Computers in Simulation (IMACS). Published by Elsevier B.V. All rights reserved.

**Keywords:** Functionally graded materials; Efficiency of thermoelectric energy converters; Figure-of-merit; Local entropy production

**1. Introduction**

In the last decade Functionally Graded Materials (FGMs) became very important in technology, especially in micro/nano-electronics, because their variation in the composition may enhance some of their properties as, for example, their efficiency in producing thermoelectric energy. Functionally graded materials of the type  $A_cB_{1-c}$ , with  $A$  and  $B$  different atomic species and  $c \in [0, 1]$  stoichiometric variable changing along a direction  $z$  inside the system, may have several applications in heat transfer problems involving nanosystems [8,15,17,26,35,44]. One of them is the heat rectification, i.e., the possibility of obtaining different values for the heat flux generated by the same temperature gradient applied in the opposite verses of a given direction. The thermal rectification can originate from various mechanisms, e.g. the different temperature dependence of the thermal conductivity at the different parts of the device, or the asymmetric transmission ratio of phonons across the interfaces inside the body. Such a phenomenon can be exploited, for instance, in the realization of thermal diodes [44]. In Ref. [22] the thermal rectification related to the geometry of the device has been investigated. The influence of the composition gradient and of a constant external heat flux on low frequency and high frequency thermal wave propagation in a system of varying stoichiometry has been studied as well.

\* Corresponding author.

E-mail addresses: [progolino@unime.it](mailto:progolino@unime.it) (P. Rogolino), [vito.cimmelli@unibas.it](mailto:vito.cimmelli@unibas.it) (V.A. Cimmelli).

**Table 1**

Values of the coefficients of expression (8) for the thermal conductivity of a nanowire of length  $L = 100\text{nm}$ , in terms of the composition from  $Ge$  to  $Si$ , at  $T = 300\text{K}$  [23].

	A	B	C	D	E	F	G	H
$L = 100\text{ nm}$	19.75	-202.51	1126.63	-3635.31	7027.22	-8009.06	4953.47	-1280.19

As far as the thermoelectric energy generators are concerned, we recall that their efficiency is defined as  $\eta = \frac{P_{el}}{\dot{Q}_{tot}}$ , where  $P_{el}$  is the electric-power output and  $\dot{Q}_{tot}$  is the heat supplied to the system per unitary time, [27,30,34]. Such an efficiency strongly depends on the so-called figure-of-merit  $Z$  [27], defined as  $Z = \frac{\epsilon^2 \sigma_e}{\lambda}$ , where  $\epsilon$  is the Seebeck coefficient,  $\sigma_e$  is the electrical conductivity, and  $\lambda$  is the thermal conductivity of the material [27]. For instance, for a thermoelectric nanowire of length  $L$ , the two sides of which are kept at the two different temperatures  $T_h$  (the hottest temperature), and  $T_c$  (the coldest temperature), with an electric current  $i$  and the total heat per unit time  $\dot{Q}_{tot}$  entering uniformly into the hot side of the element, the efficiency can be written as [27]

$$\eta = \frac{T_h - T_c}{T_h} \frac{\epsilon X [1 - (\epsilon X/Z)]}{T_h^{-1} + \epsilon X} \quad (1)$$

where

$$X \equiv \frac{iL}{\lambda(T_h - T_c)} \quad (2)$$

It follows by Eq. (1) that the higher  $Z$  the higher the efficiency of the thermoelectric generator, so that the methods to enhance  $Z$  play a fundamental role in the exploitation of FGMs properties [2,25,28]. One possible strategy is the use of nonlinear nanomaterials [14,18,21], since nonlinear effects are especially relevant at nanometric length scales [10,11,24,41]. For those systems suitable nonlinear transport equations are needed [41].

In some recent papers [39,40] we have determined the efficiency of a single homogeneous thermoelectric nanowire of length  $L$  and pointed out useful information about the way of enhancing its performances. Going a step further in our investigation, in Ref. [38] we have studied the efficiency of functionally graded  $Si_cGe_{1-c}$  nanowires as function of composition and gradient of temperature, obtaining so, for homogeneous nanowires with fixed  $c$ , the value of  $c$  which yields the best efficiency. To achieve that task we have used the following polynomial representation of the thermal conductivity

$$\lambda(c, T) = \lambda_{Ge}(T)(1 - c) + \lambda_{Si}(T)c - \sqrt{\lambda_{Si}(T)\lambda_{Ge}(T)}[Ac + Bc^2 + Cc^3 + Dc^4 + Ec^5 + Fc^6 + Gc^7 + Hc^8] \quad (3)$$

where  $\lambda_{Ge}(T)$  and  $\lambda_{Si}(T)$  are the thermal conductivities of pure  $Ge$  and  $Si$  nanowires, respectively, as functions of temperature, while  $A, B, C, D, E, F, G$ , and  $H$  are suitable temperature-dependent coefficients. Such a representation has been determined in [23] by a plot of the results in [1,16,42].

It follows by Eq. (8) that  $\lambda(0, T) = \lambda_{Ge}(T)$ . Moreover, the relation  $\lambda(1, T) = \lambda_{Si}(T)$  is satisfied under the constraint  $A + B + C + D + E + F + G + H = 0$  on the material coefficients. For the sake of illustration, in Table 1 we show the values of those coefficients, as determined in [23], for a nanowire of length  $L = 100\text{nm}$ , at  $T = 300\text{K}$ . It is easily seen by direct calculation that the previous constraint is verified.

A sketch of function  $\lambda(c)$  at  $T = 300\text{K}$ ,  $T = 400\text{K}$  and  $T = 500\text{K}$  for  $L = 100\text{nm}$  is shown in Fig. 1. It is seen that the variation of  $\lambda$  with  $c$  is steepest in the ranges  $0 \leq c \leq 0.1$  and  $0.9 \leq c \leq 1$ , since a small amount of impurities of different mass strongly contributes to phonon scattering, thus reducing very much thermal conductivity as compared with the corresponding pure system [5]. A similar curve can be obtained for  $L = 30\text{nm}$ .

In the present paper we are aimed at improving the results in [38] by determining the best fit of the experimental data for  $\lambda(c)$ . To this end, we observe that from Fig. 1 it can be argued that a more suited representation of  $\lambda(c)$  could have the form

$$\lambda(c) = ae^{f(c)} + be^{g(c)} \quad (4)$$

with  $a$  and  $b$  constant parameters, and  $f(c)$  and  $g(c)$  suitable functions of composition, all to be determined by a NLRM [6]. Then, we consider a  $Si/Ge$  graded nanowire of length  $L$ , under the action of an electric field  $\mathbf{E}$  and crossed by an electrical current  $\mathbf{i}$ , the two sides of which are kept at the two different temperatures  $T_h$  (the hottest temperature, at the right-hand side, at  $z = L$ ), and  $T_c$  (the coldest temperature, at the left-hand side, at

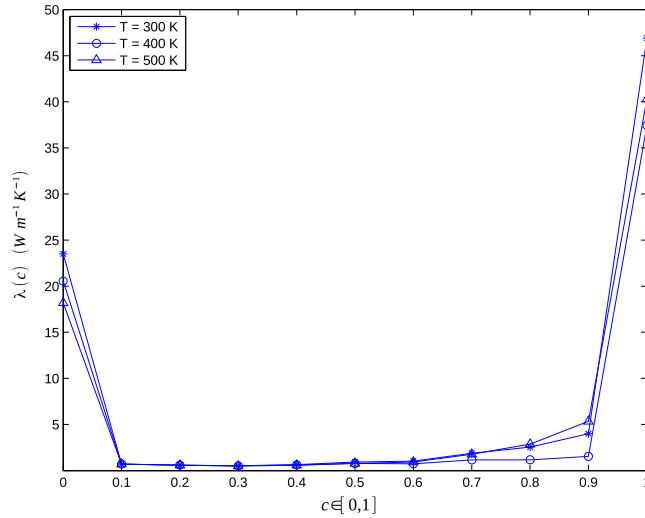


**Fig. 1.** Sketch of thermal conductivity of the alloy  $Si_cGe_{1-c}$  in terms of  $c$  at  $T = 300$  K (\*),  $T = 400$  K (o) and  $T = 500$  K ( $\Delta$ ), for  $L = 100$  nm.

$z = 0$ ). We investigate the thermoelectric efficiency of the system at hand as function of the composition and of the effective temperature gradient  $x \equiv \frac{(T_h - T_c)}{L}$ . We prove that, once the thermal conductivity is evaluated at one of the three constant temperatures  $T = 300$  K,  $T = 400$  K,  $T = 500$  K, corresponding to the experimental data at our disposal, there exists only one value  $\bar{c}$  of  $c$  in the interval  $[0, 1]$  minimizing the local rate of energy dissipation, and leading so to the best efficiency of the energy-conversion process. This value is always far-outside the interval in which the heat rectification takes place.

Owing to the result above we infer that, for the systems considered here, the best thermoelectric energy generator is constituted by a homogeneous nanowire of the type  $Si_{\bar{c}}Ge_{1-\bar{c}}$ .

The paper has the following layout.

In Section 2, we first give a sketch of the method applied to obtain the best fit of the experimental data. Then, we determine the best-fit curve representing the thermal conductivity as function of the stoichiometric variable  $c$ , at the three constant temperatures  $T = 300$  K,  $T = 400$  K, and  $T = 500$  K [23].

In Section 3, we present the mathematical model of the nonlinear thermoelectric current generator we are facing with.

In Section 4, under the hypothesis that the best efficiency corresponds to the minimum of energy dissipated, we calculate its local form and the theoretical expression giving the values of  $c$  which minimize such a rate.

In Section 5, we calculate the effective values of  $c$  corresponding to the theoretical expressions found in Section 4, i.e. the values of the composition which realize the optimal efficiency for the different temperatures. We observe that for all the temperatures these values are far-outside the interval in which heat rectification takes place, and interpret this result in view of the properties of  $\lambda(c, T)$  determined in Section 2. Possible developments of our research are discussed as well.

## 2. Thermal conductivity of graded $Si_cGe_{1-c}$ alloys

### 2.1. Best-fit procedure for thermal conductivity

The main output of a measurement is a set of experimental results which is called data. The curve fitting is the process of constructing a curve, or, equivalently, a mathematical function, that has the best fit to a series of data points, possibly subject to constraints. A related topic is the regression analysis, which focuses more on the problem of determining the error which is present in a curve that is a fit of the observed data [3]. Such an analysis leads to a fitting function or, equivalently, to a fitting curve. The mathematical function corresponding to the curve represents a relationship which describes theoretically the experimental data by using one or more parameters. The unknowns

of the problem are the parameters that quantitatively determine the fitting function as, for instance, the constants  $a$  and  $b$  in Eq. (4). That method is aimed to find the values of those parameters which allow the fitting function to match the data as closely as possible. The numerical procedure with which it is ensured the adherence of the data to a certain theoretical trend through the optimization of some parameters is called best-fit procedure. The most used method to find the curve with the best fit is the Least Squares Method (LSM) [33], which consists in minimizing the sum of the squares of the error. Thus, the best values of the parameters are those minimizing the quantity

$$\sum_i (y - y_i)^2 \quad (5)$$

where  $y = f(x)$  is a fitted value for a given point and  $y_i$  is its relative measured value. LSM is used in several contests in applied sciences. As meaningful examples let us mention the determination of the free parameters in the hazard function of human mortality and actuarial tables [13], the solution of the nonlinear population balance equation [45], the estimation of unknown parameters in the nonlinear reaction–diffusion equation [31]. Linear LSM and nonlinear LSM should be distinguished. Indeed, if the variable  $y$  is linearly dependent on the parameter, the linear LSM of minimization can be applied. If not, the nonlinear LSM of minimization must be applied. Let us remark that linearity or nonlinearity should be referred to the dependence of  $y$  on the parameters that are to be determined in order to obtain the best fit, and not to the dependence of  $y$  on the independent variable  $x$ . For instance,  $y = ae^x$  provides an example of curve which can be determined by a linear LSM method, since  $y$  is linearly dependent on the unknown parameter  $a$ . On the contrary,  $y = ae^{bx}$  represents an example of curve which requires the application of a nonlinear LSM, due to the non linear dependence of  $y$  on the unknown parameter  $b$ .

The NLRM determines values of the parameters minimizing the sum of the squares of the distances of the data points to the curve [6,32]. Therefore, if  $y_{exp}$  is the value of each data point and  $y_{fit}$  is the theoretical value of the curve, the task is to minimize the sum of squares [33]

$$\sum (y_{exp} - y_{fit})^2 \quad (6)$$

under the hypothesis of non linear dependence of the fitting curve on the parameters. Such a problem cannot be solved in one step, but it must be solved iteratively. An initial estimate of the value of each parameter is to be provided. Then, by the nonlinear regression procedure one arranges these values in order to improve the fit of the curve to the data. These iterations continue until the improvements are negligible [33].

In the present paper, by using MATHLAB ([http://www.mathlab.mtu.edu/mediawiki/index.php/Main\\_Page](http://www.mathlab.mtu.edu/mediawiki/index.php/Main_Page)), we have applied the following iterative procedure:

- as first step, we have looked for a best-fit curve represented by the equation

$$\lambda(c) = A'e^{B'c^2+D'c} + E'e^{F'c^2+G'c} \quad (7)$$

where  $A'$ ,  $B'$ ,  $D'$ ,  $E'$ ,  $F'$  and  $G'$  are the unknown parameters to be determined by NLRM;

- we have assigned an initial estimated value of each parameter entering Eq. (7);
- we have generated the curve defined by the initial values of the parameters;
- we have calculated the sum of the squares (i.e., the sum of the squares of the vertical distances of the points from the curve);
- we have adapted the parameters in such a way that the curve was as close as possible to the experimental points;
- we have stopped the calculations when we have observed a negligible difference of results in successive iterations;
- we have obtained the fit of the thermal conductivity which is shown below.

## 2.2. Constitutive equation for thermal conductivity

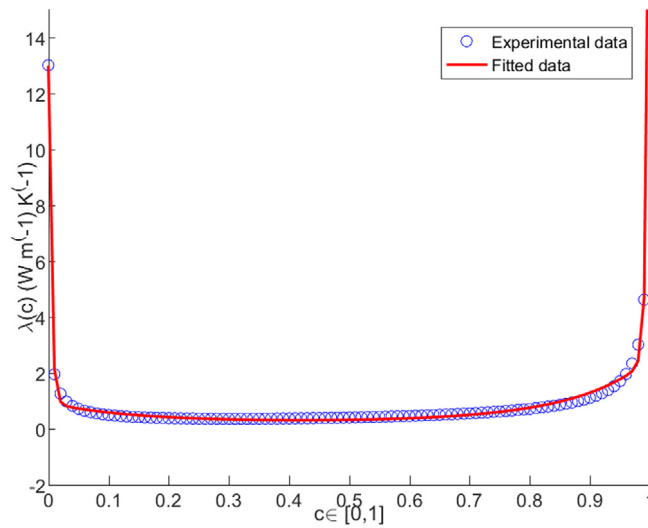
In this section we introduce a model for the thermal conductivity of graded  $Si_cGe_{1-c}$  nanowires represented by the fitting curve determined by the method described in Section 2.1. The data fitting is developed by using MATHLAB. We begin by fitting the data with the exponential function postulated in Eq. (7). The values of  $A'$ ,  $B'$ ,  $D'$ ,  $E'$ ,  $F'$  and  $G'$ , at the constant temperatures  $T = 300$  K,  $T = 400$  K,  $T = 500$  K, are shown in Table 2 (for  $L = 30$  nm), and in Table 3 (for  $L = 100$  nm). Moreover, in Figs. 2–4 are plotted the experimental and theoretical

**Table 2**Values of the parameters in Eq. (7) for the thermal conductivity of  $\text{Si}_c\text{Ge}_{1-c}$  alloys of length  $L = 30$  nm.

Temperature	A'	B'	D'	E'	F'	G'
$T = 300$ K	91.89	6.285	-5.283	12.07	229.08	-228.44
$T = 400$ K	89.74	6.21	-5.183	10.98	213.044	-212.486
$T = 500$ K	88.812	6.150	-5.119	10.17	206.73	-206.79

**Table 3**Values of the parameters in Eq. (7) for the thermal conductivity of  $\text{Si}_c\text{Ge}_{1-c}$  alloys of length  $L = 100$  nm.

Temperature	A'	B'	D'	E'	F'	G'
$T = 300$ K	1.348	6.38	-5.363	22.145	252.53	-251.94
$T = 400$ K	1.331	6.305	-5.282	19.181	239.73	-239.15
$T = 500$ K	1.309	6.208	-5.1836	16.851	228.19	-227.63

**Fig. 2.** Sketch of numerical and experimental thermal conductivity of the alloy  $\text{Si}_c\text{Ge}_{1-c}$  in terms of  $c$  at temperature  $T = 300$  K, for  $L = 30$  nm. (For interpretation of the references to colour in this figure legend, the reader is referred to the web version of this article.)

functions of  $\lambda(c, T)$  given by Eq. (7), at  $T = 300$  K,  $T = 400$  K and  $T = 500$  K, for a nanowire of length  $L = 30$  nm. In Figs. 5–7 the experimental data are plotted for a nanowire of length  $L = 100$  nm. Comparison of Fig. 1 with Figs. 5–7 leads to the following conclusions:

- the qualitative behavior of function  $\lambda(c)$  given by Eqs. (7) and (8) is the same;
- both representations evidence the existence of two dilute zones, close to  $c = 0$  and  $c = 1$  respectively, in which the variation of  $\lambda$  is rather steep, while  $\lambda$  is almost constant between these two zones;
- in Figs. 5–7 the range of steep variation of  $\lambda$  is more narrow with respect to that in Fig. 1;
- it is evident in Figs. 5–7 that in the two dilute zones close to  $c = 0$  and  $c = 1$  the variation of  $\lambda$  is more steep with respect to that shown in Fig. 1 in the same zones. This is a further proof of what we already observed in Section 1, i.e. that a small amount of impurities of different mass strongly contributes to phonon scattering, thus reducing very much thermal conductivity as compared with the corresponding pure system [5].

Finally, a further comparison of the red and blue curves in Figs. 2–7 shows that the best-fit curve reproduces with satisfactory accuracy the distribution of the experimental data.

For the constitutive equation (7) the following constraints on the coefficients

$$\lambda(0) = A' + E' = \lambda_{Ge} \quad \lambda(1) = A'e^{B'+D'} + E'e^{F'+G'} = \lambda_{Si} \quad (8)$$

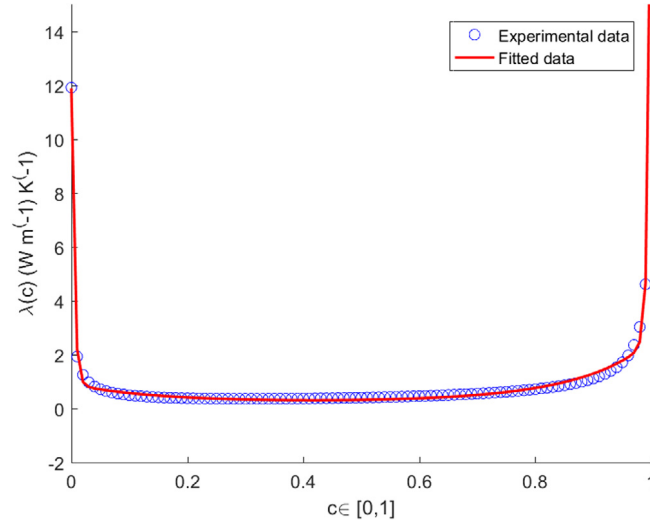


**Fig. 3.** Sketch of numerical and experimental thermal conductivity of the alloy  $Si_cGe_{1-c}$  in terms of  $c$  at temperature  $T = 400$  K, for  $L = 30$  nm. (For interpretation of the references to colour in this figure legend, the reader is referred to the web version of this article.)

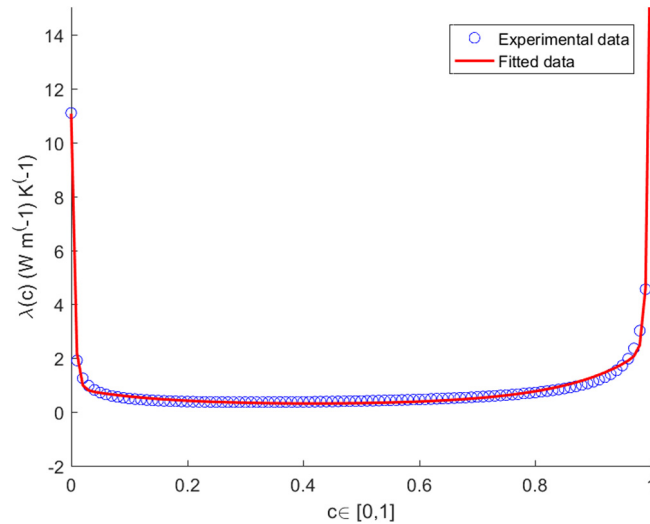


**Fig. 4.** Sketch of numerical and experimental thermal conductivity of the alloy  $Si_cGe_{1-c}$  in terms of  $c$  at temperature  $T = 500$  K, for  $L = 30$  nm. (For interpretation of the references to colour in this figure legend, the reader is referred to the web version of this article.)

are expected to hold, whatever is the value of the temperature  $T$ . Accordingly, not all parameters  $A'$ ,  $B'$ ,  $D'$ ,  $E'$ ,  $F'$  and  $G'$  are independent, and only 4 parameters, together with the measured values of  $\lambda_{Ge}$  and  $\lambda_{Si}$ , are necessary. However, we found that the representation with 4 parameters introduces an error on the fit which is higher with respect to that with 6 parameters, and hence we preferred to use the more reliable representation with 6 parameters. It is worth remarking that Eq. (7) has been obtained by fitting the experimental data, and hence it represents those data only within a certain approximation. As a consequence, also the relations in Eq. (8) are verified with a certain approximation. For the sake of comparison, in Table 4 we quote the experimental values of  $\lambda_{Ge}$  and  $\lambda_{Si}$ , together with the corresponding values of  $A' + E'$  and  $A'e^{B'+D'} + E'e^{F'+G'}$ , respectively. It can be seen that the relations (8) are satisfied with a very good approximation.

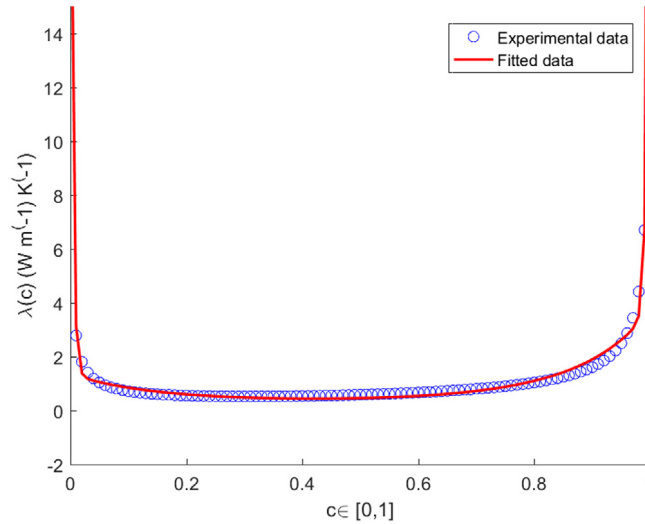


**Fig. 5.** Sketch of numerical and experimental thermal conductivity of the alloy  $Si_cGe_{1-c}$  in terms of  $c$  at  $T = 300$  K, for  $L = 100$  nm. (For interpretation of the references to colour in this figure legend, the reader is referred to the web version of this article.)

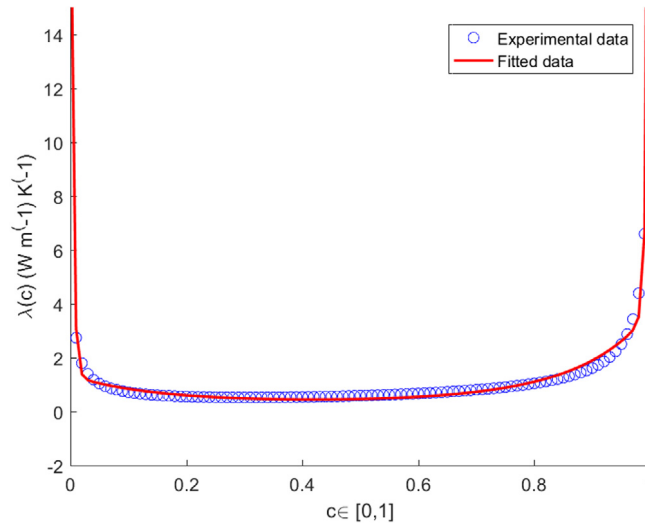


**Fig. 6.** Sketch of numerical and experimental thermal conductivity of the alloy  $Si_cGe_{1-c}$  in terms of  $c$  at  $T = 400$  K, for  $L = 100$  nm. (For interpretation of the references to colour in this figure legend, the reader is referred to the web version of this article.)

**Table 4**

Experimental values of the thermal conductivity (in  $W\ m^{-1}\ K^{-1}$ ) for pure  $Ge$  and pure  $Si$  (from [28]), compared with the quantities  $A' + E'$  and  $A'e^{B'+D'} + E'e^{F'+G'}$ , respectively, at  $T = 300$  K,  $T = 400$  K and  $T = 500$  K, for  $L = 100$  nm.

	$\lambda_{Ge}$	$A' + E'$	$\lambda_{Si}$	$A'e^{B'+D'} + E'e^{F'+G'}$
$T = 300$ K	23.50	23.49	43.58	43.67
$T = 400$ K	20.54	20.51	38.16	37.97
$T = 500$ K	18.19	18.16	33.40	33.14

### 3. Nonlinear heat transport in one-dimensional nanosystems

Let us consider a graded  $Si_cGe_{1-c}$  nanowire of length  $L$  under the action of an electric field  $\mathbf{E}$ , and crossed by an electrical current  $\mathbf{i}$ . The two sides of the nanowire are kept at the two different temperatures  $T_h$  (the hottest

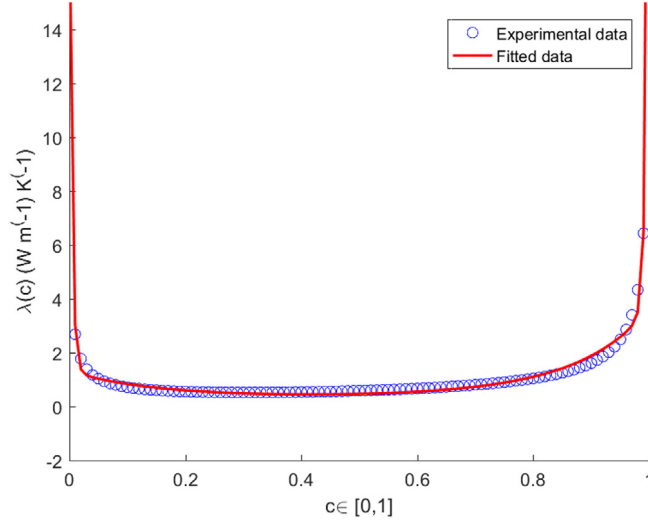


**Fig. 7.** Sketch of numerical and experimental thermal conductivity of the alloy  $Si_cGe_{1-c}$  in terms of  $c$  at  $T = 500$  K, for  $L = 100$  nm. (For interpretation of the references to colour in this figure legend, the reader is referred to the web version of this article.)

temperature, at  $z = L$ ), and  $T_c$  (the coldest temperature, at  $z = 0$ ). We assume that both the electric current  $\mathbf{i}$  and the total heat per unit time  $\dot{Q}_{\text{tot}}$  enter uniformly into the hot side of the element at the right-hand side of the generator.

A nonlinear model for such a system has been developed in [39], where the local balance of energy

$$\rho \frac{du}{dt} + \nabla \cdot \mathbf{q} = \mathbf{E} \cdot \mathbf{i} \quad (9)$$

with  $\rho$  as the mass density,  $u$  as the specific internal energy and  $\mathbf{q}$  as the heat flux, has been closed by the constitutive equations

$$\mathbf{q} = -\nabla \mathbf{q} \cdot \mathbf{l} - \lambda (1 - b) \nabla T + \Pi \mathbf{i} \quad (10a)$$

$$\mathbf{i} = -\sigma_e \epsilon \nabla T + \sigma_e \mathbf{E} \quad (10b)$$

where  $\mathbf{l}$  denotes a characteristic-length vector accounting for the order of magnitude of the physical dimension of the system,  $b$  is a dimensionless quantity smaller than 1, and  $\Pi$  is the Peltier coefficient [27,41].

We develop our analysis under the hypothesis that both  $\mathbf{q}$  and  $\mathbf{E}$  depend only on the position on the longitudinal axis  $z$ , as well as that  $\mathbf{q}$  and  $\mathbf{i}$  are parallel. Then, in steady states, Eq. (9) yields

$$\nabla \cdot \mathbf{q} = \frac{\partial q(z)}{\partial z} = \mathbf{E} \cdot \mathbf{i}$$

The previous relation allows to write

$$\nabla \mathbf{q} \cdot \mathbf{l} = \frac{\partial q(z)}{\partial z} \mathbf{l} \cong \bar{E} \bar{l} \mathbf{i} \quad (11)$$

where  $\bar{E}$ , and  $\bar{l}$  denote the mean values of  $|\mathbf{E}|$ , and  $|\mathbf{l}|$  on the interval  $[0, L]$ , respectively. Finally, by coupling of Eqs. (10a) and (11) we obtain the nonlinear constitutive equation for the heat flux

$$\mathbf{q} = -[\lambda (1 - b) + \sigma_e \epsilon (\Pi - \bar{E} \bar{l})] \nabla T + \sigma_e (\Pi - \bar{E} \bar{l}) \mathbf{E} \quad (12)$$

On the other hand, second law of thermodynamics imposes that the local rate of entropy production

$$\sigma_s = \rho \frac{ds}{dt} + \nabla \cdot \frac{\mathbf{q}}{T} \quad (13)$$

with  $s$  as the entropy density and  $\frac{\mathbf{q}}{T}$  as the entropy flux, is nonnegative for arbitrary thermodynamic processes.



Under the constitutive assumption  $s = s(u)$ , once the Gibbs relation  $\frac{ds}{dt} = \frac{ds}{du} \frac{du}{dt} = \frac{1}{T} \frac{du}{dt}$  is used, and account is taken of Eq. (9), one obtains

$$\sigma_s = \frac{1}{T} \left( -\frac{\mathbf{q}}{T} \cdot \nabla T + \mathbf{E} \cdot \mathbf{i} \right) \quad (14)$$

By multiplying Eq. (14) by  $T$  we obtain the local rate of energy dissipated along the process in the form

$$T\sigma_s = \mathbf{E} \cdot \mathbf{i} - \frac{\nabla T}{T} \cdot \mathbf{q} \quad (15)$$

To proceed further, we use Eqs. (10b) and (12) in order to eliminate  $\mathbf{E}$  and  $\mathbf{q}$  in the right-hand side of Eq. (15), getting so

$$T\sigma_s = \frac{i^2}{\sigma_e} + i[\epsilon T_h - (\Pi - \bar{E} \bar{l})] \nabla T + \lambda(1-b)(\nabla T)^2 \quad (16)$$

Thus, the nonlinear constitutive equation (12) is physically admissible, i.e., it is compatible with second law of thermodynamics, if, and only if, the right-hand side of Eq. (16) is always nonnegative [9]. Such a compatibility has been proved in Ref. [39] by applying the classical Onsager procedure [12].

#### 4. Maximization of thermoelectric efficiency

In this section we exploit Eq. (16) in order to investigate the efficiency of the system at hand as thermoelectric energy converter. To this end, following the way already paved in [38], we apply a new procedure based on the mathematical analysis of the local rate of entropy production (or, equivalently, of energy dissipation) along the thermoelectric process. Indeed, our basic hypothesis is that the best efficiency corresponds to a minimum of the rate of energy dissipated. This is plausible from the physical point of view, since the thermoelectric efficiency is related to the level of irreversibility induced by the thermal and electrical transport. Eq. (16) provides an explicit form of the local rate of energy dissipated, which depends on the temperature gradient and on the thermal conductivity  $\lambda(c, T)$ . Thus, once  $\lambda$  is evaluated at one of the three constant temperatures considered above, i.e.  $T = 300$  K,  $T = 400$  K,  $T = 500$  K, the quantity  $T\sigma_s$  depends only on the temperature gradient and on the composition  $c$ .

Taking into account that we are facing with a one-dimensional system, and assuming that the direction of the temperature gradient is parallel to the longitudinal direction  $z$ , we make the approximation  $\nabla T \simeq \frac{T_h - T_c}{L}$  and put

$$x \equiv \sqrt{\frac{T_h - T_c}{L}} \quad (17)$$

In this way, the right-hand side of Eq. (16) takes the form

$$\mathcal{E}(c, x) \equiv T\sigma_s = \frac{i^2}{\sigma_e} + i[\epsilon T_h - (\Pi - \bar{E} \bar{l})]x^2 + \lambda(c)(1-b)x^4 \quad (18)$$

In order to obtain the couples  $(c, x)$  corresponding to the optimal efficiency, we must calculate the minima (if any) of the right-hand side of Eq. (18).

To this end, first we determine the stationary points for  $\mathcal{E}(c, x)$  as solutions of the algebraic system

$$\frac{\partial \mathcal{E}}{\partial c} = \frac{d\lambda}{dc}(1-b)x^4 = 0 \quad (19a)$$

$$\frac{\partial \mathcal{E}}{\partial x} = 2i[\epsilon T_h - (\Pi - \bar{E} \bar{l})]x + 4\lambda(c)(1-b)x^3 = 0 \quad (19b)$$

Since  $x$  is a strictly positive quantity, by direct calculations we see that the stationary points  $(c_{opt}, x_{opt})$  of the function  $\mathcal{E}(c, x)$  correspond to the values  $c_{opt}$  satisfying the relation  $\frac{d\lambda}{dc} = 0$ , with

$$x_{opt} = \sqrt{\frac{-i[\epsilon T_h - (\Pi - \bar{E} \bar{l})]}{4\lambda_{opt}(1-b)}} \quad (20)$$

wherein  $\lambda_{opt} = \lambda(c_{opt})$ . These points exist provided the inequality

$$i[\epsilon T_h - (\Pi - \bar{E} \bar{l})] < 0 \quad (21)$$

**Table 5**

Values of  $\lambda_{opt}$  (in  $\text{W m}^{-1} \text{K}^{-1}$ ) corresponding to the compositions  $c_{opt}$  at  $T = 300 \text{ K}$ ,  $T = 400 \text{ K}$  and  $T = 500 \text{ K}$ , for  $L = 30 \text{ nm}$ .

Temperature (K)	$c_{opt}$	$\lambda_{opt}$ (in $\text{W m}^{-1} \text{K}^{-1}$ )
$T = 300$	0.420342	30.2719
$T = 400$	0.417311	30.4308
$T = 500$	0.416179	30.6095

holds. It is worth observing that Eq. (21) represents a unilateral constraint on the physical parameters entering the problem.

Let us now calculate the second derivatives of  $\mathcal{E}$ , and let us analyze their sign. We get

$$\frac{\partial^2 \mathcal{E}}{\partial c^2} = \frac{d^2 \lambda}{dc} (1 - b) x^4 \quad (22a)$$

$$\frac{\partial^2 \mathcal{E}}{\partial x^2} = 2i[\epsilon T_h - (\Pi - \bar{E} \bar{l})] + 12\lambda x^2 (1 - b) \quad (22b)$$

$$\frac{\partial^2 \mathcal{E}}{\partial c \partial x} = 4x^3 \frac{d\lambda}{dc} (1 - b) \quad (22c)$$

We see that  $\partial^2 \mathcal{E} / \partial c^2$  is positive if, and only if, the second derivative of  $\lambda$  with respect to  $c$  is positive, i.e. in  $c_{opt}$   $\lambda$  attains a minimum. Moreover, since  $\frac{d\lambda}{dc}$  vanishes in correspondence of the solution  $(c_{opt}, x_{opt})$ , also  $\partial^2 \mathcal{E} / \partial c \partial x$  vanishes in correspondence of such a solution. Then, in order to allow the determinant of the Hessian matrix of  $\mathcal{E}(c, x)$  to be positive, it is necessary and sufficient that  $\partial^2 \mathcal{E} / \partial x^2$  is positive. This is true under the further constraint

$$2i[\epsilon T_h - (\Pi - \bar{E} \bar{l})] + 12\lambda_{opt} x_{opt}^2 (1 - b) > 0 \quad (23)$$

On the other hand, due to the constraint (21), the first term in Eq. (23) is negative. However, the second term is positive, so that the constraints (21) and (23) are compatible.

By the analysis above it follows that the points of best efficiency are those in which  $\lambda$  attains a minimum.

## 5. Results and discussion

In this section we discuss the solutions of the system of Eqs. (19a)–(19b), which have been calculated by using MATHEMATICA (<https://www.wolfram.com/mathematica/>). First, we analyze the solutions obtained for a nanowire of length  $L = 30 \text{ nm}$  at the constant temperatures  $T = 300 \text{ K}$ ,  $T = 400 \text{ K}$  and  $T = 500 \text{ K}$ .

At  $T = 300 \text{ K}$ ,  $\mathcal{E}(c, x)$  attains a minimum for  $c = 0.420342$ . In correspondence of this point we obtain  $\lambda = 30.2719 \text{ W m}^{-1} \text{K}^{-1}$ .

At  $T = 400 \text{ K}$  the value in which  $\mathcal{E}(c, x)$  attains a minimum is  $c = 0.417311$ . In this point  $\lambda = 30.4308 \text{ W m}^{-1} \text{K}^{-1}$ .

Finally, at  $T = 500 \text{ K}$   $\mathcal{E}(c, x)$  is minimum for  $c = 0.416179$  and  $\lambda = 30.6095 \text{ W m}^{-1} \text{K}^{-1}$ .

The previous results are summarized in Table 5.

Let us now consider a nanowire of length  $L = 100 \text{ nm}$  at the same temperatures.

At  $T = 300 \text{ K}$  the minimum value of  $\mathcal{E}(c, x)$  is achieved when  $c = 0.420306$ . In correspondence of this point  $\lambda = 0.436811 \text{ W m}^{-1} \text{K}^{-1}$ .

At  $T = 400 \text{ K}$  we get a minimum for  $\mathcal{E}(c, x)$  at  $c = 0.418874$  and in this point  $\lambda = 0.440293 \text{ W m}^{-1} \text{K}^{-1}$ .

At  $T = 500 \text{ K}$  we get minimum of  $\mathcal{E}(c, x)$   $c = 0.417494$  and the corresponding value of  $\lambda$  is  $0.443616 \text{ W m}^{-1} \text{K}^{-1}$ . These results are summarized in Table 6.

We observe that there are marked differences with respect to the results obtained in [38]. In fact, in [38] we obtained several minima of  $\lambda$ , corresponding to different values of the stoichiometric variable.

Moreover, one of them were close to the first dilute zone. Thus, we supposed that, for different temperature and length of the nanowire, the best efficiency could be obtained in the same zone where the rectification takes place. In the present case, instead, no one of the local minima of  $\lambda$  is reached in the two narrow dilute intervals close to  $c = 0$  and  $c = 1$ , and this seems to indicate that optimal efficiency and rectification cannot be achieved in the same

**Table 6**

Values of  $\lambda_{opt}$  (in  $\text{W m}^{-1} \text{K}^{-1}$ ) corresponding to the compositions  $c_{opt}$  at  $T = 300 \text{ K}$ ,  $T = 400 \text{ K}$  and  $T = 500 \text{ K}$ , for  $L = 100 \text{ nm}$ .

Temperature (K)	$c_{opt}$	$\lambda_{opt}$ (in $\text{W m}^{-1} \text{K}^{-1}$ )
$T = 300$	0.420306	0.436811
$T = 400$	0.418874	0.440293
$T = 500$	0.417494	0.443616

range of values of the stoichiometric variable. As a consequence, one cannot use the same nanowire to obtain both thermoelectric energy conversion and rectification of the heat flux.

Moreover, at the three different temperatures considered here, both for  $L = 30 \text{ nm}$  and  $L = 100 \text{ nm}$  there are only three points of minimum, very close each other, corresponding also to small differences in  $\lambda$ , perhaps due to the experimental error on the data. This substantial coincidence of the minima proves that the nonlinear regression analysis carried out in Section 2.2 is correct and the fitting function is stable with respect to small variations of the data.

It is worth observing that, for  $L = 30 \text{ nm}$   $\lambda$  is two orders of magnitude higher than  $\lambda$  for  $L = 100 \text{ nm}$ . Thus, taking present the expression of  $Z$ , we conclude that at this scale, the efficiency seems to decrease with  $L$ . In fact, as already observed in [38], if one goes to smaller and smaller  $L$ , the value of  $\lambda(c, T)$  must be replaced by the effective size-dependent thermal conductivity, since a reduction in  $L$  implies a reduction in  $\lambda(T, c)$ , because the phonon–walls collisions are more relevant as compared to phonon–phonon collisions or phonon–impurity collisions, [5].

A logical extension of the present paper would be to consider the composition dependence not only of the thermal conductivity but also of the electrical conductivity  $\sigma_e$  and of the Seebeck coefficient  $\epsilon$ , since an increasing of  $Z$  can also be achieved by increasing the so called “power factor”, i.e., the product  $\epsilon^2 \sigma_e$ . In literature one can find several experimental studies on the dependency on composition of such quantities (see, for instance, [29,36,37]). However, how to achieve that task is a delicate problem from the practical point of view, since the experimental values of  $\epsilon$  and  $\sigma_e$  are not independent. For instance, it is possible to increase the electrical conductivity by increasing the carrier density, but in this way the Seebeck coefficient decreases [19,20].

Another aspect of interest for future research would be to find the composition of the  $\text{Si}/\text{Ge}$  alloy optimizing the power output [27]

$$P_{el} = \int_L^0 i E d\xi \quad (24)$$

of the thermoelectric nanowire rather than the efficiency. Indeed, power optimization is a current topic of research [4,7,43], since in some situations one is interested to get a very high power output rather than the best efficiency.

Finally, the thermoelectric efficiency in the bulk ( $L \simeq 1 \text{ mm}$  or more) should be analyzed as well.

## Acknowledgments

P. R. acknowledges the financial support of the Italian National Group of Mathematical Physics (GNFM-INdAM) and of the University of Messina, Italy under grant FFABR 2019.

V. A. C. acknowledges the financial support of the Italian National Group of Mathematical Physics (GNFM-INdAM), and of the University of Basilicata, Italy under grants RIL 2013 and RIL 2015.

This paper contains in extended form the results presented by one of the authors (V. A. C.) at the 15th MEETING ON APPLIED SCIENTIFIC COMPUTING AND TOOLS (MASCOT2018). V. A. C. thanks the Chair and the Co-Chair of the Conference, Dr. Rosa Maria Spitaleri and Prof. Sandra Carillo, for their friendly hospitality.

## References

- [1] B. Abeles, D. Beers, G. Cody, J. Dismukes, Thermal conductivity of Ge-Si alloys at high temperatures, *Phys. Rev.* 125 (1962) 44–46.
- [2] A. Balandin, K.L. Wang, Effect of phonon confinement on the thermoelectric figure of merit of quantum wells, *J. Appl. Phys.* 84 (1998) 6149, (5 pages).
- [3] J.W. Caim, *Mathematics of Fitting Scientific Data*, in: E. Bell (Ed.), *Molecular Life Sciences*, Springer, New York, NY, 2014.
- [4] C. Calaza, I. Donmez, M. Salleras, G. Gadea, J.D. Santos, A. Morata, A. Tarancón, L. Fonseca, Optimization of power output in planar thermoelectric microgenerators based on Si nanowires, *J. Phys. Conf. Ser.* 773 (2016) 012026, (4 pages).

- [5] I. Carlomagno, V. Cimmelli, D. Jou, Heat flux rectification in graded  $Si_cGe_{1-c}$ : longitudinal and radial heat flows, *Physica E* 90 (2017) 149–157.
- [6] S. Chatterjee, A.S. Hadi, Regression Analysis by Example, fifth ed., Wiley, Hoboken, 2012.
- [7] Y. Chen, M. He, J. Tang, G.C. Bazan, Z. Liang, Flexible thermoelectric generators with ultrahigh output power enabled by magnetic field-aligned metallic nanowires, *Adv. Electron. Mater.* 4 (2018) 1800200, (6 pages).
- [8] V.A. Cimmelli, Different thermodynamic theories and different heat conduction laws, *J. Non-Equilib. Thermodyn.* 34 (2009) 299–333.
- [9] V.A. Cimmelli, D. Jou, T. Ruggeri, P. Ván, Entropy principle and recent results in non-equilibrium theories, *Entropy* 16 (2014) 1756–1807.
- [10] V.A. Cimmelli, A. Sellitto, D. Jou, Nonlocal effects and second sound in a nonequilibrium steady state, *Phys. Rev. B* 79 (2009) 014303, (13 pages).
- [11] V.A. Cimmelli, A. Sellitto, D. Jou, Nonequilibrium temperatures heat waves and nonlinear heat transport equations, *Phys. Rev. B* 81 (2010) 054301, (9 pages).
- [12] S.R. De Groot, P. Mazur, Nonequilibrium Thermodynamics, North-Holland Publishing Company, Amsterdam, 1962.
- [13] X. Feng, G. Heb, Abdurishit, Estimation of parameters of the Makeham distribution using the least squares method, *Math. Comput. Simulation* 77 (2008) 34–44.
- [14] D.K. Ferry, S.M. Goodnick, Transport in Nanostructures, second ed., Cambridge University Press, Cambridge, England, 2009.
- [15] Y. Gelbstein, Z. Dashevsky, M. Dariel, High performance n-type PbTe-based materials for thermoelectric applications, *Physica B* 363 (2005) 196–205.
- [16] C. Glassbrenner, G. Slack, Thermal conductivity of Silicon and Germanium from 3° K to the melting point, *Phys. Rev.* 134 (1964) 1058–1069.
- [17] E. Gonzalez-Noya, D. Srivastava, M. Menon, Heat-pulse rectification in carbon nanotube Y junctions, *Phys. Rev. B* 79 (2009) 115432, (5 pages).
- [18] K.E. Goodson, M.I. Flik, Electron and Phonon Thermal Conduction in Epitaxial high- $T_c$  Superconducting Films, *J. Heat Trans. - T. ASME* 115 (1993) 17–25.
- [19] J.P. Heremans, Low-dimensional thermoelectricity, *Acta Phys. Pol. A* 1008 (2005) 609–634.
- [20] J.P. Heremans, C.M. Thrush, D.T. Morelli, Thermopower enhancement in lead telluride nanostructures, *Phys. Rev. B* 70 (2004) 115334, (5 pages).
- [21] G. Joshi, H. Lee, Y. Lan, X. Wang, G. Zhu, D. Wang, R.W. Gould, D.C. Cuff, M.Y. Tang, M.S. Dresselhaus, G. Chen, Z. Ren, Enhanced thermoelectric figure-of-merit in nanostructured p-type Silicon Germanium bulk alloys, *Nano Lett.* 8 (2008) 4670–4674.
- [22] D. Jou, I. Carlomagno, V. Cimmelli, A thermodynamic model for heat transport and thermal wave propagation in graded systems, *Physica E* 73 (2015) 242–249.
- [23] D. Jou, I. Carlomagno, V. Cimmelli, Rectification of low-frequency thermal waves in graded  $Si_cGe_{1-c}$ , *Phys. Lett. A* 380 (2016) 1824–1829.
- [24] D. Jou, J. Casas-Vázquez, G. Lebon, Extended Irreversible Thermodynamics, fourth revised ed., Springer, Berlin, 2010.
- [25] V.L. Kuznetsov, Functionally graded materials for termoelectric applications, in: D.M. Rowe (Ed.), *Thermoelectrics Handbook: Macro To Nano – Sec. Vol. 38*, CRC Press, Boca Raton, 2005.
- [26] G. Lebon, Heat conduction at micro and nanoscales: A review through the prism of Extended Irreversible Thermodynamics, *J. Non-Equilib. Thermodyn.* 39 (2014) 35–59.
- [27] G. Lebon, D. Jou, J. Casas-Vázquez, Understanding Nonequilibrium Thermodynamics, Springer, Berlin, 2008.
- [28] D. Li, Y. Wu, P. Kim, L. Shi, P. Yang, A. Majumdar, Thermal conductivity of individual silicon nanowires, *Appl. Phys. Lett.* 83 (2003) 2934–2936.
- [29] E. Macía, Thermoelectric figure of merit of AlPdRe icosahedral quasicrystals: Composition-dependent effects, *Phys. Rev. B* 69 (2004) 184202, (7 pages).
- [30] N. Mingo, Thermoelectric figure of merit and maximum power factor in III-V semiconductor nanowires, *Appl. Phys. Lett.* 84 (2004) 2652, (3 pages).
- [31] C. Mocenni, D. Madeo, E. Sparacino, Linear least squares parameter estimation of nonlinear reaction diffusion equations, *Math. Comput. Simulation* 81 (2011) 2244–2257.
- [32] J.H. Motulsky, A. Christopoulos, Fitting Models To Biological Data using Linear and Nonlinear Regression, Oxford University Press, 2004.
- [33] J.H. Motulsky, A.L. Ransnas, Fitting curves to data using nonlinear regression: A practical and nonmathematical review, *The FASEB J.* 1 (1987) 365–374.
- [34] G.S. Nolas, J. Sharp, H.J. Goldsmid, Thermoelectrics: Basic Principles and New Materials Developments, Springer, New York, 2001.
- [35] A.O. Olatunji-Ojo, S.K.S. Boetcherb, T.R. Cundaria, Thermal conduction analysis of layered functionally graded materials, *Comput. Mater. Sci.* 54 (2012) 329–335.
- [36] S. Perumal, S. Gorsse, U. Ail, R. Decourt, A.M. Umarji, Effect of composition on thermoelectric properties of polycrystalline  $CrSi_2$ , *J. Electron. Mater.* 42 (2013) 1042–1046.
- [37] D. Ravinder, P.V.B. Reddy, Temperature and composition dependence of thermoelectric power studies of copper-substituted lithium ferrites, *Mater. Lett.* (2003).
- [38] P. Rogolino, V. Cimmelli, Thermoelectric efficiency of graded  $Si_cGe_{1-c}$  alloys, *J. Appl. Phys.* 124 (2018) 094301, (6 pages).
- [39] P. Rogolino, A. Sellitto, V. Cimmelli, Influence of nonlinear effects on the efficiency of a thermoelectric generator, *Z. Angew. Math. Phys.* 66 (2015) 2829–2842.
- [40] P. Rogolino, A. Sellitto, V.A. Cimmelli, Influence of the electron and phonon temperature and of the electric-charge density on the optimal efficiency of thermoelectric nanowires, *Mech. Res. Commun.* 68 (2015) 77–82.

- [41] A. Sellitto, V.A. Cimmelli, D. Jou, *Mesoscopic Theories of Heat Transport in Nanosystems*, Springer, Berlin, 2016.
- [42] M. Steele, F. Rosi, Thermal conductivity and thermoelectric power of germanium-silicon alloys, *J. Appl. Phys.* 29 (1958) 1517–1520.
- [43] C.C. Wu, S. Kumarakrishnan, T.O. Mason, Thermopower composition dependence in ferrosinels, *J. Solid State Phys.* 37 (1981) 144–150.
- [44] N. Yang, G. Zhang, B. Li, Carbon nanocone: A promising thermal rectifier, *Appl. Phys. Lett.* 93 (2008) 243111, (3 pages).
- [45] Z. Zhu, C.A. Dorao, H.A. Jakobsen, A least-squares method with direct minimization for the solution of the breakage-coalescence population balance equation, *Math. Comput. Simulation* 79 (2008) 716–727.